

**BENDING BEHAVIOUR OF TRIANGULAR WEB PROFILE  
STEEL BEAM SECTION**

**NOR SALWANI BINTI HASHIM**

**UNIVERSITI SAINS MALAYSIA**

**2012**

**BENDING BEHAVIOUR OF TRIANGULAR WEB PROFILE  
STEEL BEAM SECTION**

**by**

**NOR SALWANI BINTI HASHIM**

**Thesis submitted in fulfillment of the requirements**

**for the Degree of**

**Master of Science**

**May 2012**

**KELAKUAN LENTUR BAGI KERATAN KELULI DENGAN WEB  
BERBENTUK SEGITIGA**

**oleh**

**NOR SALWANI BINTI HASHIM**

**Tesis yang diserahkan untuk  
memenuhi keperluan bagi  
Ijazah Sarjana**

**Mei 2012**

## ACKNOWLEDGEMENTS

Praise to Allah, The Most Gracious, Most Merciful, with His permission, Alhamdulillah this report has completed.

First and foremost, I would like to convey my heartfelt gratitude and highest appreciation to Dr. Fatimah De'nan, for being my supervisor, because she always gives constant guide, advice, support, brilliant ideas and constructive comments throughout the preparation of this research.

To my beloved parents and also my siblings, special thanks for their commitment, encouragement and patient throughout the whole duration of research and the continued support. Without their continuous words of encouragement, it would be difficult to complete this thesis.

My sincere and special thanks also to my beloved friends and classmates for being supportive and for their contributions at various occasions received all this while. Last but not least, thank you to all that have contributed either directly or indirectly in making this study success. Lastly, I would like to acknowledge and extend my heartfelt gratitude to the Ministry of Higher Education for financial support that has made the completion of this thesis possible. Thank you.

# TABLE OF CONTENTS

	<b>Page</b>	
<b>ACKNOWLEDGEMENTS</b>	ii	
<b>TABLE OF CONTENTS</b>	iii	
<b>LIST OF TABLES</b>	vii	
<b>LIST OF FIGURES</b>	x	
<b>LIST OF SYMBOLS</b>	xiv	
<b>LIST OF ABBREVIATIONS</b>	xvi	
<b>ABSTRAK</b>	xvii	
<b>ABSTRACT</b>	xviii	
 <b>CHAPTER 1 – INTRODUCTION</b>		
1.1	General	1
1.2	Problem Statement	6
1.3	Objectives	9
1.4	Scope of Work	9
1.5	Organisation of Thesis	10

## CHAPTER 2 – LITERATURE REVIEW

2.1	Introduction	12
2.2	Summary	29

## CHAPTER 3 – NUMERICAL STUDY

3.1	Introduction	30
3.2	Basic Equations	30
3.3	Finite Element Analysis on the Bending of Triangular Web Profile Steel Section	
	3.3.1 Modelling	37
	3.3.2 Meshing	37
	3.3.3 Loading and Boundary Condition	39
	3.3.4 Convergence Study	39
3.4	Parametric Study	
	3.4.1 Effect of the Web Thickness, $t_w$	42
	3.4.2 Effect of the Depth of Web, $D$	46
	3.4.3 Effect of the Corrugation Angle, $\theta$	50

3.4.4	Effect of loading position	55
3.5	Determination on the second moment of area of $T_{RI}WP$ in term of FW steel section	60
3.6	Discussion	66

## **CHAPTER 4 – EXPERIMENTAL STUDY**

4.1	Introduction	67
4.2	Tensile Test	67
4.3	Bending Test Equipment and Set-Up	69
4.4	Test Procedures	75
4.5	Determination on the second moment of area of $T_{RI}WP$ in term FW steel section	76
4.6	Discussion	83

## **CHAPTER 5 – CONCLUSION**

5.1	Conclusion	85
5.2	Recommendations for Future Studies	86

<b>REFERENCES</b>	87
-------------------	----

**APPENDIXES**

Appendix A	92
Appendix B	93
Appendix C	94
Appendix D	95
Appendix E	96



## LIST OF TABLES

		<b>Page</b>
Table 1.1	The most common types of beam (McKenzie, 1998)	1
Table 3.1	The dimensional properties of models for convergence study	40
Table 3.2	Data of maximum nodal displacements with different mesh sizes	40
Table 3.3	Deflection due to the effects of web thickness, $t_w$ under point load 14 kN about major axis and 3 kN about minor axis (Section $200 \times 100 \times 6 \times t_w$ mm)	43
Table 3.4	Deflection due to the effects of web thickness, $t_w$ under point load 8 kN about major axis and 1 kN about minor axis (Section $180 \times 75 \times 5 \times t_w$ mm)	43
Table 3.5	Deflection due to the effects of depth of web, $D$ under point load 14 kN about major axis and 3 kN about minor axis (Section $D \times 100 \times 6 \times 3$ mm)	47
Table 3.6	Deflection due to the effects of depth of web, $D$ under point load 8 kN about major axis and 1 kN about minor axis (Section $D \times 75 \times 5 \times 2$ mm)	47
Table 3.7	Deflection due to the effects of corrugation angle, $\theta$ under point load 14 kN about major axis and 3 kN about minor axis (Section $200 \times 100 \times 6 \times 3$ mm)	52
Table 3.8	Deflection due to the effects of corrugation angle, $\theta$ under point load 8 kN about major axis and 1 kN about minor axis (Section $180 \times 75 \times 5 \times 2$ mm)	52

Table 3.9	Deflection due to the effects of loading position under point load 14 kN about major axis and 3 kN about minor axis (Section 200×100×6×3 mm)	57
Table 3.10	Deflection due to the effects of loading position under point load 8 kN about major axis and 1 kN about minor axis (Section 180×75×5×2 mm)	57
Table 3.11	The dimensional properties of models for analysis	80
Table 3.12	Deflections for T <sub>RI</sub> WP1 and FW1 steel section	62
Table 3.13	Deflections for T <sub>RI</sub> WP2 and FW2 steel section	62
Table 3.14	Percentage differences of flexural stiffness for T <sub>RI</sub> WP1 and FW1 steel section	63
Table 3.15	Percentage differences of flexural stiffness for T <sub>RI</sub> WP2 and FW2 steel section	65
Table 4.1	Dimensions of T <sub>RI</sub> WP and FW steel section specimens in experimental study	68
Table 4.2	Dimension of flat test specimens	69
Table 4.3	Tensile test results	70
Table 4.4	The dimensional properties of models for testing	77
Table 4.5	Deflections for T <sub>RI</sub> WP1 and FW1 steel section	78
Table 4.6	Deflections for T <sub>RI</sub> WP2 and FW2 steel section	79

Table 4.7	Percentage differences of flexural stiffness for T <sub>RI</sub> WP1 and FW1 steel section	80
Table 4.8	Percentage differences of flexural stiffness for T <sub>RI</sub> WP2 and FW2 steel section	83

## LIST OF FIGURES

		<b>Page</b>
Figure 1.1	The corrugated web I-beams for both columns and girders (Zeman and Co, 1999)	3
Figure 1.2	A typical shape of trapezoid web section (Tahir et al., 2008)	4
Figure 1.3	Shape and dimensions of a typical $T_{RI}WP$ steel section (all units are in mm)	5
Figure 1.4	Transition model from TWP steel section to $T_{RI}WP$ steel section	8
Figure 1.5	A typical diagram of x-axis and y-axis	8
Figure 2.1	Dimensions of test specimens and corrugation profiles (Elgaaly et al., 1997)	13
Figure 2.2	Corrugation profiles (Chan et al., 2002)	16
Figure 2.3	Geometry of the models tested experimentally (Khalid et al., 2004)	17
Figure 2.4	Types of loading positions (Luo and Edlund, 1996a)	19
Figure 2.5	A steel girder with trapezoidally corrugated webs under patch loading (Luo and Edlund, 1996a)	20
Figure 2.6	A plate girder with trapezoidally corrugated webs in shear (Luo and Edlund, 1996b)	21

Figure 2.7	Structural character of the WCW H-beam (Zhang et al., 2000; Li et al., 2000)	23
Figure 2.8	Geometric parameters of trapezoidally corrugated web (Yi et al., 2008)	25
Figure 2.9	Profile of I-girder with corrugated webs (Moon et al., 2009)	27
Figure 2.10	Geometry of the test specimen (Elgaaly and Seshadri, 1997)	28
Figure 3.1	Load-deflection relationships	31
Figure 3.2	Triangular Web Profile ( $T_{RI}WP1$ ) Steel Section (Section 200x100x6x3)	33
Figure 3.3	Triangular Web Profile ( $T_{RI}WP2$ ) Steel Section (Section 180x75x5x2)	34
Figure 3.4	Flat Web (FW1) Steel Section (Section 200x100x6x3)	35
Figure 3.5	Flat Web (FW2) Steel Section (Section 180x75x5x2)	36
Figure 3.6	Typical modeling of a $T_{RI}WP$ steel section	37
Figure 3.7	Meshing of a $T_{RI}WP$ steel section for one cycle	38
Figure 3.8	Deflection mode of a $T_{RI}WP$ steel section model	39
Figure 3.9	Graph of maximum nodal displacement at mid span against number of element	41

Figure 3.10	Geometric parameters of a $T_{RI}WP$ steel section	42
Figure 3.11	Plot of deflection, $\delta$ versus web thickness, $t_w$ (Section $200 \times 100 \times 6 \times t_w$ mm)	44
Figure 3.12	Plot of deflection, $\delta$ versus web thickness, $t_w$ (Section $180 \times 75 \times 5 \times t_w$ mm)	45
Figure 3.13	Plot of deflection, $\delta$ versus depth of web, $D$ (Section $D \times 100 \times 6 \times 3$ mm)	48
Figure 3.14	Plot of deflection, $\delta$ versus depth of web, $D$ (Section $D \times 75 \times 5 \times 2$ mm)	49
Figure 3.15	Types of corrugation angles	51
Figure 3.16	Plot of deflection, $\delta$ versus corrugation angles, $\theta$ (Section $200 \times 100 \times 6 \times 3$ mm)	53
Figure 3.17	Plot of deflection, $\delta$ versus corrugation angles, $\theta$ (Section $180 \times 75 \times 5 \times 2$ mm)	54
Figure 3.18	Types of loading position	56
Figure 3.19	Plot of deflection, $\delta$ versus loading position (Section $200 \times 100 \times 6 \times 3$ mm)	58
Figure 3.20	Plot of deflection, $\delta$ versus loading position (Section $180 \times 75 \times 5 \times 2$ mm)	59
Figure 3.21	Load, $P$ versus deflection, $\delta$ for $T_{RI}WP1$ and $FW1$ steel section	64

Figure 3.22	Load, $P$ versus deflection, $\delta$ for T <sub>RI</sub> WP2 and FW2 steel section	66
Figure 4.1	The tensile test sample as per ASTM: A370-03a	69
Figure 4.2	Typical view for every type of specimen	72
Figure 4.3	The test instrument arrangement	73
Figure 4.4	The actual test set up (FW section 200×100×6×3 mm)	74
Figure 4.5	The actual test set up (T <sub>RI</sub> WP section 200×100×6×3 mm)	76
Figure 4.6	The position of LVDTs for the bending test (all units in mm)	77
Figure 4.7	Load, $P$ versus deflection, $\delta$ for FW1 and T <sub>RI</sub> WP1 steel section	79
Figure 4.8	Load, $P$ versus deflection, $\delta$ for FW2 and T <sub>RI</sub> WP2 steel section	82

## LIST OF SYMBOLS

$t_w$	Web thickness
$t_f$	Flange thickness
$B$	Flange width
$D$	Overall depth
$d$	Depth of web
$\theta$	Corrugation angle
$h_r$	Corrugation thickness
$H$	Corrugation amplitude
$I$	Second moment of area
$\lambda$	Cycle length ratio
$\sigma_{zz}$	Bending stresses
$P$	Concentrated load
$\delta$	Deflection
$\lambda_s$	Shear buckling parameter
$C_{w,co}$	Warping constant
$d_{avg}$	Average corrugation depth



$M_p$	Plastic moment of resistance
$M_e$	Elastic moment of resistance
$M$	Elastic moment of resistance
$\rho_y$	Design strength
$Z_{xx}$	Elastic section modulus
$S_{xx}$	Plastic section modulus
$\sigma$	Elastic stress
$\delta$	Vertical deflection at mid span
$E$	Young's modulus
$\nu$	Poisson's ratio
$P$	Concentrated load
$c$	Length of loading

## LIST OF ABBREVIATIONS

T <sub>RI</sub> WP1	Triangular Web Profile Steel Section (200×100×6×3 mm)
T <sub>RI</sub> WP2	Triangular Web Profile Steel Section (180×75×5×2 mm)
TWP	Trapezoidal Web Profile Steel Section
FW1	Flat web (200×100×6×3 mm)
FW2	Flat web (180×75×5×2 mm)
UB	Universal beam
HPS	High Performance Steels
PW <sub>x</sub>	Plane Web
HC1R <sub>x</sub>	Horizontal one arc corrugation
VCR <sub>x</sub>	Vertical arcs corrugation
HC2R <sub>x</sub>	Horizontal two arcs corrugation
WCW	Wholly corrugated web
3D	Three-dimensional
QTS	Quadrilateral thick shell element
TTS	Triangular thick shell element
LVDT	Low voltage displacement transducers

# **KELAKUAN LENTUR BAGI KERATAN KELULI DENGAN WEB BERBENTUK SEGITIGA**

## **ABSTRAK**

Rasuk dan galang yang beralur telah digunakan secara meluas dalam industri bangunan, gudang atau dalam pembinaan jambatan bagi jalan raya dan kereta api. Dalam usaha untuk memaksimum penggunaan beban berbanding dengan keratan keluli web rata (FW), keratan keluli yang dikenali sebagai profil web berbentuk segitiga ( $T_{RIWP}$ ) telah dikaji. Keratan keluli  $T_{RIWP}$  terdiri daripada dua plat bebibir yang disambungkan kepada plat web berbentuk segitiga. Kajian ini adalah tentang prestasi lentur dalam paksi utama ( $I_x$ ) dan paksi sekunder ( $I_y$ ) bagi keratan keluli  $T_{RIWP}$  dibandingkan dengan keratan keluli FW. Penyelidikan ini mengandungi dua peringkat iaitu analisis unsur terhingga dan ujian makmal. Kajian ini melibatkan enam model keratan keluli FW sebagai spesimen kawalan dan enam model keratan keluli  $T_{RIWP}$  yang masing-masing bersaiz  $200 \times 100 \times 6 \times 3$  mm dan  $180 \times 75 \times 5 \times 2$  mm. Daripada keputusan analisis unsur terhingga dan ujian makmal, boleh diperhatikan bahawa pesongan dalam paksi sekunder bagi keratan keluli  $T_{RIWP}$  adalah lebih rendah daripada keratan keluli FW. Ini bermakna keratan keluli  $T_{RIWP}$  lebih kukuh berbanding keratan keluli FW dalam paksi sekunder. Sementara itu, pesongan dalam paksi utama bagi keratan keluli  $T_{RIWP}$  adalah lebih tinggi berbanding dengan keratan keluli FW. Ini bermaksud, pada paksi utama, keratan keluli FW adalah lebih kukuh daripada keratan keluli  $T_{RIWP}$ . Ia boleh disimpulkan bahawa keratan keluli web berbentuk segitiga memberikan kesan kepada kelakuan rasuk untuk merintang lenturan.

# **BENDING BEHAVIOUR OF TRIANGULAR WEB PROFILE STEEL BEAM SECTION**

## **ABSTRACT**

Corrugated beams and girders are widely used in industrial buildings, warehouses or in bridge constructions for road and rail. In order to assure that the steel section can resist more loads compared to that of flat web steel section (FW), a new steel section known as triangular web profile ( $T_{RI}WP$ ) steel section has been studied. A  $T_{RI}WP$  steel section is a built-up steel section consisting of two flanges connected to a web plate with a triangular profile. This thesis described the study on the bending behaviour about major ( $I_x$ ) and minor ( $I_y$ ) axes of  $T_{RI}WP$  compared to that of flat web (FW) steel sections. This research consists of two main stages namely finite element analysis and laboratory testing. The study involved six models of FW steel section as control specimens and six models of  $T_{RI}WP$  steel sections of size  $200 \times 100 \times 6 \times 3$  mm and  $180 \times 75 \times 5 \times 2$  mm, respectively. From the finite element and laboratory testing results, it was observed that the deflection about minor axis for  $T_{RI}WP$  steel section is less than FW steel section. It means the  $T_{RI}WP$  steel section was stiffer compared to that of FW steel section about minor axis. Meanwhile, the deflections about major axis for  $T_{RI}WP$  steel section was more than that of FW steel section. Its means the FW was stiffer than  $T_{RI}WP$  steel section about major axis. It was concluded that the triangular web of steel section contributed much effects in the behaviour of the beam to resist bending.

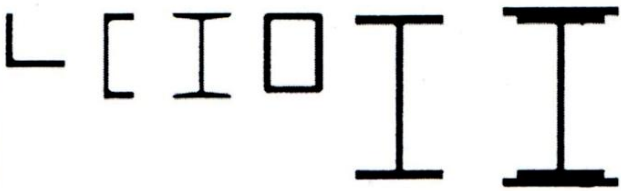
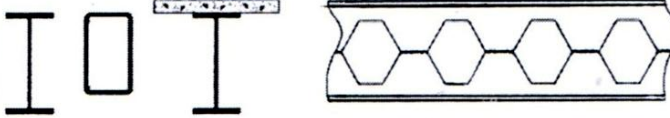

# CHAPTER 1

## INTRODUCTION

### 1.1 General

Beam is a structural element which is most frequently used in structural design. The main function of a beam is to transfer vertical loading to adjacent structural elements and finally to the foundations (McKenzie, 1998). The most common types of beam with an indication of the span range for which they may be appropriate are given in Table 1.1.

Table 1.1 The most common types of beam (McKenzie, 1998)

Span	Beam Types
1	 <p style="text-align: center;">Angle   Channel   Joist   Tube   Universal beam   Compound</p>
1	 <p style="text-align: center;">UB   RHS   Composite beams   Castellated beams</p>
15 -	 <p style="text-align: center;">Castellated beams   Welded plate girders   Welded box girders</p>

In many instances, it is necessary to support heavy vertical loads over long spans resulting large bending moments and shear forces. If the magnitude of bending moments and shear forces is large, then it is necessary to fabricate a beam utilizing plates welded together into an I-shaped section. The primary purpose of the flange plate is to resist the tensile and compressive forces induced by the bending moment. While, the primary purposes of the web plate is to resist the shearing forces (McKenzie, 1998). These sections are normally more efficient in terms of steel weight than rolled sections, particularly when variable depth girders are used because it can be designed to suit the requirements.

If the span or magnitude of loading required that larger and deeper sections are used, castellated beams formed by welding together with profiled cut UB sections, plate girders or box girders and corrugated plate in which the web and flanges are individual plates welded together can be fabricated. The corrugated plate is used in structural component in aircraft, ships, offshore structures, bridges and buildings. Corrugated webs used in beams have been employed in bridges in France and Japan for several years and the corrugated steel web have found comprehensive application in long-span roof beams in Sweden (Usman, 2001).

Zeman and Co in Vienna, one of the Austrian companies is produced economical built-up girders consisting of plate flanges welded to a corrugated web. Engineers have long realized that corrugations in webs enormously increase their stability against buckling and affect the costing of the design. Thus, corrugated web I-Beams have the potential to eliminate the cost of web stiffeners (Figure 1.1). In addition, the use of thinner webs may used less raw material cost with savings estimated at 10%-30% compared with conventional built-up sections and more than 30% compared with

standard I-beams. Corrugated web I-beam provide high strength to weight ratio and reduce the depth of steel when compared to truss systems. As the clear span increase, the costs also can be reduced. The higher resistance against rotation also reduces the need of brace angles or tubes. The minimum length of a corrugated web I-beam is 6 m and the maximum length is 20 m (Zeman and Co, 1999).



Figure 1.1 The corrugated web I-beams for both columns and girders (Zeman and Co, 1999)

Modern plate girders are normally fabricated by welding together two flanges and a web plate to form an I-section. Such girders are capable of carrying more loads over longer spans and generally using standard rolled sections or compound girders. Plate girders are typically used as long-span floor girders in buildings, as bridge girders, and as crane girders in industrial structures. Normally a plate girder may not be require until the span exceeds 25 m and recently numerous plate girders spanning 60 m to 100 m have been constructed (Clarke and Coverman, 1987). Therefore, stiffeners are used to reinforce the web.

Nowadays, the corrugated webs are introduced to allow the use of thin plates without stiffeners for buildings and bridges. It could eliminate the usage of larger thickness and stiffeners that contribute to the reduction in beam weight and cost.

Steel construction in Malaysia usually used steel web I-beam and H-column rather than non uniform section such as trapezoidal web profile (TWP) or corrugated web. However, steel beam with trapezoid web profile (Figure 1.2) have been widely used in recent years (Elgaaly et al., 1995; Chan et al., 2002; Atan, 2001) because the demand of steel as a construction material increases since it has become a popular construction material. The purpose of using TWP sections is to take advantage of the benefits offered by the sections which has thin and corrugated web (Tahir et al., 2008).

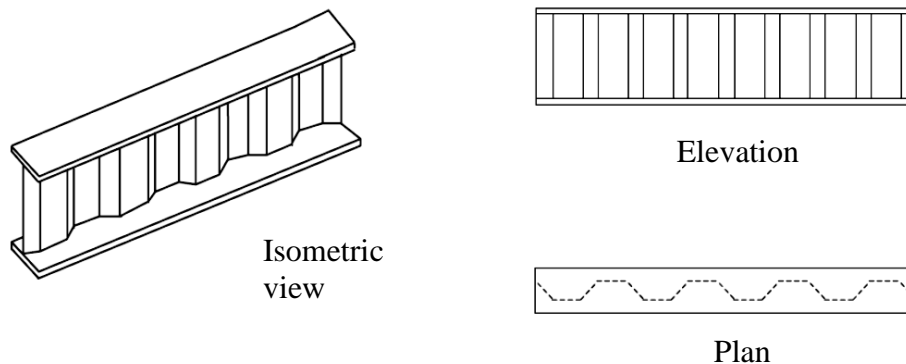


Figure 1.2 A typical shape of trapezoid web section (Tahir et al., 2008)

In Malaysia, the technology was introduced by Trapezoid Web Profile Sdn. Bhd. based in Pasir Gudang. Trapezoid Web Profile Sdn. Bhd., subsidiary of the Johor Heavy Industries Group of Companies, was incorporated on 25th September 1995 as part of the policies to manufacturing activities of TWP steel section for construction (Usman, 2001). In the absence of any specific design guide, the British Standard (BS 5950-1, 2000) can be applied as a basic design for a corrugated steel section. However,



simplification and conservativeness must be carried out because the general design considerations are limited to flat web steel section and there is no special provision for TWP in BS5950-1:2000.

A triangular web profile ( $T_{RI}WP$ ) steel section is a section made of two flanges connected to a slender web. The web and the flanges can be produced from different steel grades depending on design requirements. The flanges width and thickness is determined based on the depth of the section. The web is corrugated at regular interval into triangular shape along the length of the beam. Figure 1.3 shows the shape and the dimensions of a typical section of  $T_{RI}WP$  steel system.

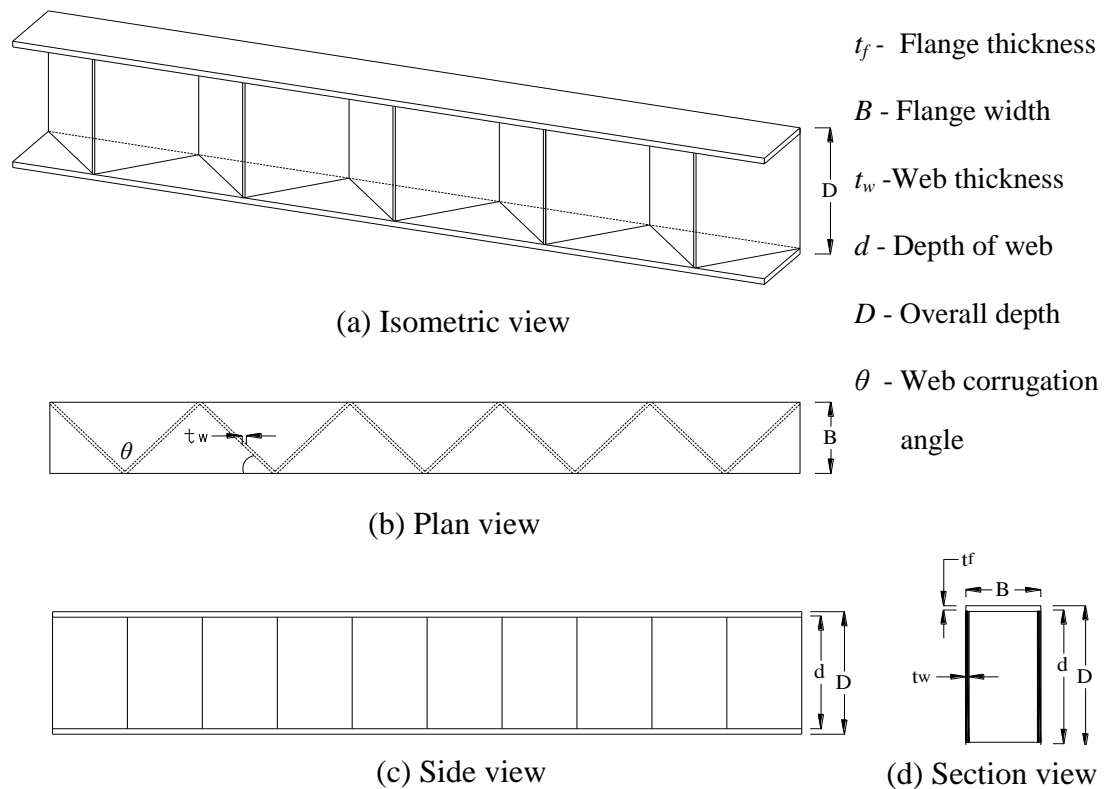


Figure 1.3 Shape and dimensions of a typical  $T_{RI}WP$  steel section (all units are in mm)

The purpose of this study is to examine bending behaviour about minor and major axes for  $T_{RI}WP$  in comparison with FW steel section. Finite element analysis and laboratory testing have been conducted. The hypothesis of this research was that the  $T_{RI}WP$  maybe able to resist bending better than FW steel section.

## **1.2 Problem Statement**

The structural action of a beam is predominantly bending, with other effects such as shear and bearing also present. In addition to ensure that beams have sufficient capacities to resist these effects, it is important that the stiffness properties are adequate to avoid excessive deflection of the cross section.

According to the previous study (Luo and Edlund, 1996a), the highest value of strength obtained when the girder with trapezoidal web is loaded at the centre of the oblique part (of corrugation). Meanwhile, the girder has the lowest strength when it is applied at the centre of the flat part. In order to increase the bending behaviour of corrugated steel section, a new shape of steel section known as triangular web profile ( $T_{RI}WP$ ) steel section have been studied in this research.

This triangular web profile ( $T_{RI}WP$ ) steel section eliminated the use of eccentric stiffeners as used in trapezoidal web profile (TWP) steel section. The transition model from trapezoidal web profile (TWP) steel section to triangular web profile ( $T_{RI}WP$ ) steel section are shown in Figure 1.4. This type of steel section was used to study the bending behaviour about minor and major axes by finite element analysis and laboratory testing.

The second moment of area is one of the important elements because it give affects bending behaviour. The second moment of area value can be easily calculated for a normal FW steel section because the web is flat and uniform in profile throughout the

length. But, for a  $T_{RI}WP$  steel section, second moment of area calculation is difficult to calculate due to the corrugated shape of web. For the current application and conservative solution, the web profile is neglected when calculating the second moment of area, assuming it does not bring a significant contribution towards the buckling strength (Elgaaly et al., 1997). However, other researchers found that the web contributed to the increase in the second moment of area (Atan, 2001; Tan, 2004). Therefore, it is important to know the calculation method of the second moment of area for  $T_{RI}WP$  steel section.

In steel design, the second moment of area about y-y axis,  $I_y$  (see Figure 1.5) value is important either in structural safety or to increase the efficiency of the section. In British Standard 5950- Part 1:2000, the basic derivation of the second moment of area,  $I_y$  in terms of the geometry of cross sections is already available for I-beam section. However, this formula is not suitable for other corrugated sections such as the  $T_{RI}WP$  steel section. It is the purpose of the thesis to report on the finite element analysis and laboratory testing carried out to obtain the second moment of area value,  $I_y$  of a member of  $T_{RI}WP$  specimens. The determination of the second moment of area,  $I_y$  value of  $T_{RI}WP$  steel section in term of,  $I_y$  of the FW steel section is clearly described in this thesis.

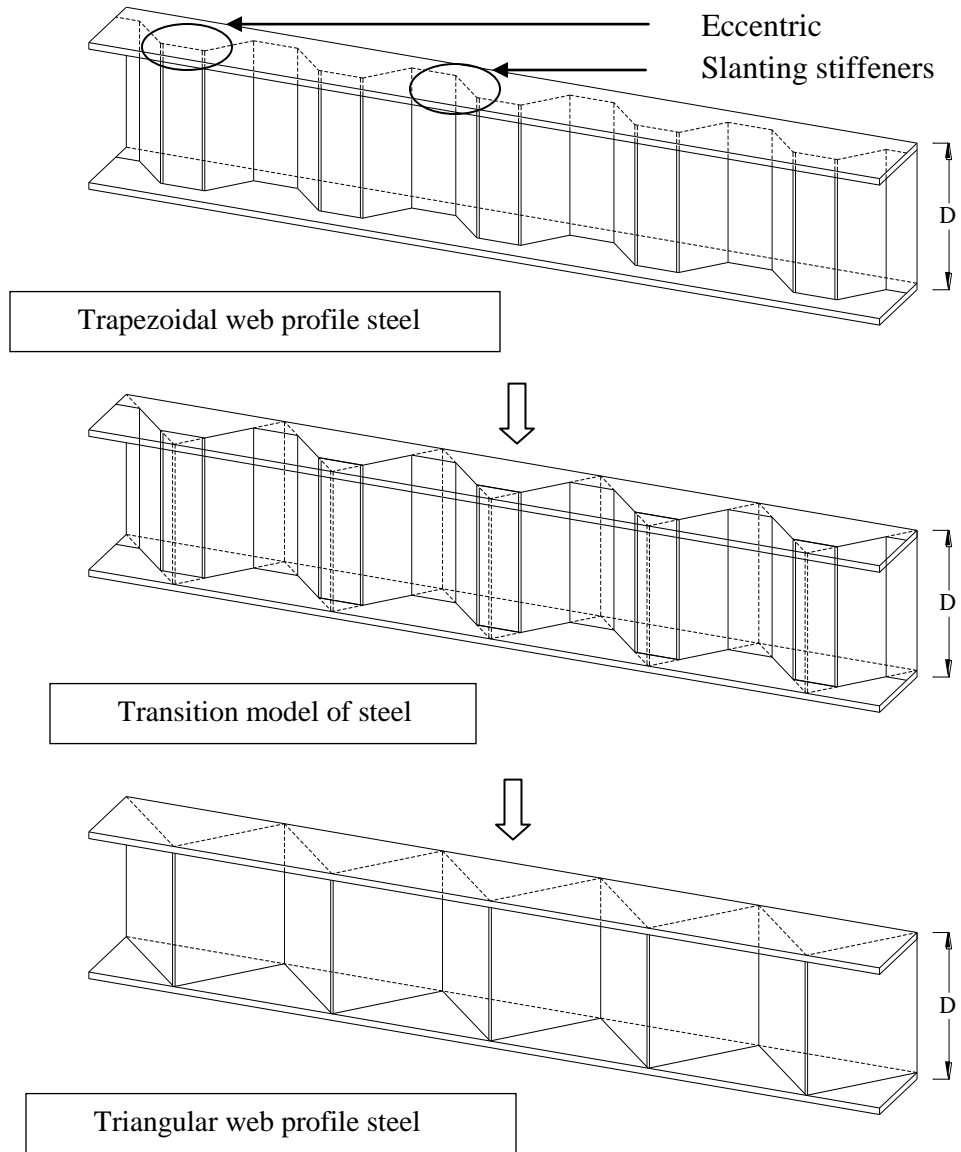


Figure 1.4 Transition model from TWP steel section to  $T_{RI}WP$  steel section

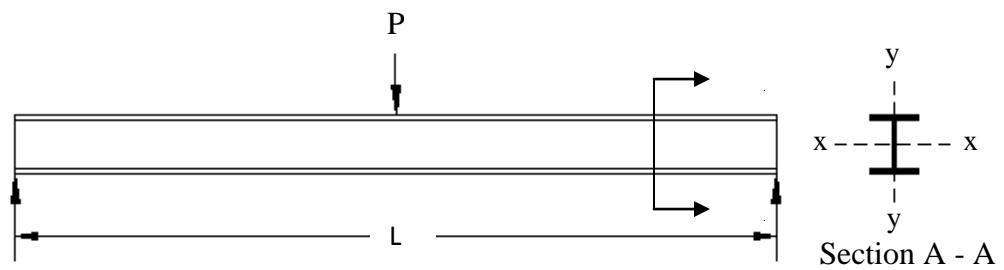


Figure 1.5 A typical diagram of x-axis and y-axis

The hypothesis of this research was that the  $T_{RI}WP$  maybe able to resist bending better than FW steel section. This is due to the greater value of the second moment of area in minor axis,  $I_y$  of  $T_{RI}WP$  steel section. Thus, the assumption done by previous researchers (Elgaaly et al., 1997) who neglected the web when calculate the second moment of area is imprecise.

### **1.3 Objectives**

The objectives of this research are:

- a) To study the bending behaviour of  $T_{RI}WP$  steel section by finite element analysis.
- b) To perform parametric study of  $T_{RI}WP$  steel section by finite element analysis.
- c) To verify the bending behaviour of  $T_{RI}WP$  steel section by laboratory testing.

### **1.4 Scope of Work**

This study focused mainly on finite element analysis and laboratory testing for  $T_{RI}WP$  subject to bending behaviour. FW steel section is used as the control specimen for this research. The scope of work can be divided into several important parts:

- a) Determination of specimen sizes for FW and  $T_{RI}WP$  steel section.
- b) The FW and  $T_{RI}WP$  steel section specimens were analysed using LUSAS software. This involved the finite element analysis on the effect of the web thickness, effect of the depth of web, effect of the corrugation angle and effect of the loading position.

- c) Then laboratory testing was performed to obtain the second moment of area,  $I_x$  and  $I_y$  for the FW and T<sub>RI</sub>WP steel sections. Bending tests included six specimens (three sizes of FW as control specimens and three sizes of T<sub>RI</sub>WPs steel section with two types of dimensions) were used. Each of beam section was tested using several spans such as 3 m, 4 m and 4.8 m. In total, 24 sets of readings were collected. The test involved two types of sizing, namely 180×75×5×2 mm and 200×100×6×3 mm section. All bending tests were carried out at elastic loading to obtain the elastic relationship between the load and deflection of the beams. Later, the data from both types of the beam were compared.
- d) The results obtained in modelling with LUSAS software and laboratory testings were then compared.
- e) Lastly, the ratios of the  $I_x$  and  $I_y$  values in term of  $I_x$  and  $I_y$  of FW for the two sections (i.e FW and T<sub>RI</sub>WP steel section) by finite element analysis and laboratory testing were determined.

## **1.5 Organisation of Thesis**

This thesis consists of five chapters. Chapter 1 consists of the introduction and overview of the research. A review of the relevant literatures is given in Chapter 2 where the review of past researches on corrugated section such as bending capacity, lateral torsional buckling and design procedure are presented.

Chapter 3 presents method of the analysis about the bending behaviour of T<sub>RI</sub>WP steel section about major and minor axes compared to that of FW steel section.

Chapter 4 deals with the laboratory testing work of T<sub>RI</sub>WP steel section compared to that of FW steel section.

Chapter 5 summarises the important conclusions of the study. Important areas for future research are also recommended.

## CHAPTER 2

### LITERATURE REVIEW

#### 2.1 Introduction

A number of tests have been conducted by previous researchers to investigate various mechanical properties of TWP steel section such as moment capacity, flange capacity, shear buckling strength, axial buckling and deflection (Usman, 2001; Tahir et al., 2008; Atan, 2001; Tan, 2004; De'nan, 2008; Yew, 2007). Studies on the behavior of beam with trapezoid web profile have been conducted since the early 60's and only since 1980 the full capacity of trapezoid web profile plates has been studied in greater detail (Johnson and Cafolla, 1997b; Elgaaly et al., 1997).

In the mid-90s, Advanced Technology for Large Structural Systems (ATLSS) Center at Lehigh University and Modjeski and Masters, Inc., with funding by the Federal Highway Administration, began studying on non-traditional steel bridge beam configurations. The study involved on the selecting of optimum corrugated shape (trapezoidal or sinusoidal) by considering structural performance, fabrication, and manufacturing processes. This corrugated shape was designed to replace the routine box and I-girder shapes, and it was found that the strength and ability of HPS (High Performance Steels) corrugated shapes would increase web stability, allow for reduction in web thickness without the web stiffeners and more benefits in fabrication and erection (Wilson, 1992).

The early studies have been done by Elgaaly et al. (1995) which are focused on the vertically trapezoidal corrugation. The failure mechanisms of beams with corrugated web under different loading modes such as bending mode, shear mode and compressive patch loads were investigated. It was found that the failure of beams under shear loading



is due to local buckling on the web for coarse corrugation and global buckling on the web for dense corrugation (Elgaaly et al., 1996). The contribution of the web profile could be neglected in the calculation of the second moment of area of the TWP section, due to its contribution towards the beam load-carrying capability. Six specimens of corrugated webs in the center panel and flat panels adjacent to the support were tested experimentally. The entire specimens were cross braced to ensure that the failure would occur in the center panel. The dimension and the test setup are shown in Figure 2.1. All the specimens tested failed due to flange yielding followed by vertical buckling of the compression flange into the web (Elgaaly et al., 1997).

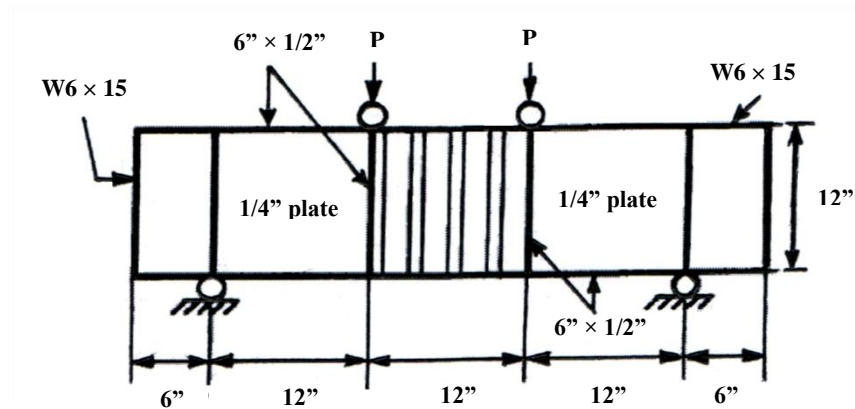


Figure 2.1 Dimensions of test specimens and corrugation profiles (Elgaaly et al., 1997)

The test results indicate that the contribution of the web to the bending capacity of the beam could be neglected because the corrugated web has no stiffness perpendicular to the direction of the corrugation, except for a very small distance that is adjacent to and restrained by the flanges. Thus its contribution could be neglected and the ultimate moment capacity is based on the flange yield stress. The test specimens were modeled using ABAQUS program to perform nonlinear finite element analysis.

The finite element model was able to show the test results to a very good degree of accuracy. It was concluded that the moment capacity increases with the increase of the ratio between the plastic and yield stresses of the flange material (Elgaaly et al., 1997).

However, the web might have contribution towards increasing the second moment of area (Atan, 2001; Tan, 2004). An experimental investigations, theoretical analysis and finite element analysis were carried out using LUSAS finite element software to study the flexural behavior of trapezoid corrugated web sections. From the theoretical analysis, the deflection values, bending stresses and ultimate moment capacities for trapezoid corrugated sections were found to be approximately equalled to normal FW sections. This was expected since all calculations were performed by neglecting the web contribution. However, from the finite element analysis and experimental investigation, the deflection of trapezoid corrugated section was found to be 12% higher than that of the normal FW section. It indicated that the elastic behavior of the trapezoid corrugated web section was more stiffens compared to the ordinary normal FW section in flexure and that the web contribution cannot be ignored in calculating the elastic flexural properties and ultimate moment for the trapezoid corrugated web section.

Besides that, analytical and experimental studies on 300×120×10×2 mm TWP section were performed by Tan (2004) to determine the second moment of area about its minor axis ( $I_y$ ). Compared to FW section, it was found that the corrugation thickness ( $h_r$ ) to section width ( $B$ ) ratio has a significant effect on the buckling load for the TWP section. On the other hand, increasing the depth of section ( $D$ ) would not change its compression resistance. Nevertheless, under compressive patch loads, two distinct modes of failure were observed. These involve the formation of collapse mechanism on

flange followed by the web crippling or yielded web cripples followed by vertical bending of the flange into the crippled web. The failure of these beams is found to be dependent on the loading position and corrugation parameters where it can be a combination of the aforementioned modes (Elgaaly and Seshadri, 1997).

The effect of web corrugation on the strength of beam has been studied by Chan et al. (2002). Beams with plane web, vertically and horizontally corrugated webs were modelled and analysed using LUSAS finite element package where material non-linear elastic-plastic behavior has been considered. The corrugation profiles studied are half circle corrugation, which is shown in Figure 2.2. For the horizontally corrugated case, one arc and two arcs were studied, while half-circular (22.41 mm mean radius) wave corrugation was used for the vertical type. Three different radius corrugations were taken for each type of the beam to investigate its effect on the strength of beam. Ordinary I-beams, with plane web, were also tested experimentally. I-beam of 500 mm length, 75 mm flange width and 127 mm deep were selected to be the basis for investigation. The comparison between the results obtained from both methods, for the plane web type, shows 3.1% to 7.1% differences and for the beams with vertically corrugated web stands 38.8% to 54.4% higher moments than the horizontal type. The vertically corrugated web provides a good resistance against the flange buckling, compared to the plane and horizontally corrugated web types and the same results for the other three radiuses. Moreover, corrugated web beams with larger corrugation radius could resist higher bending moment and it is true for the sizes used. The vertically corrugated beam had a 10.6% reduction in weight when compared with the beam with FW.

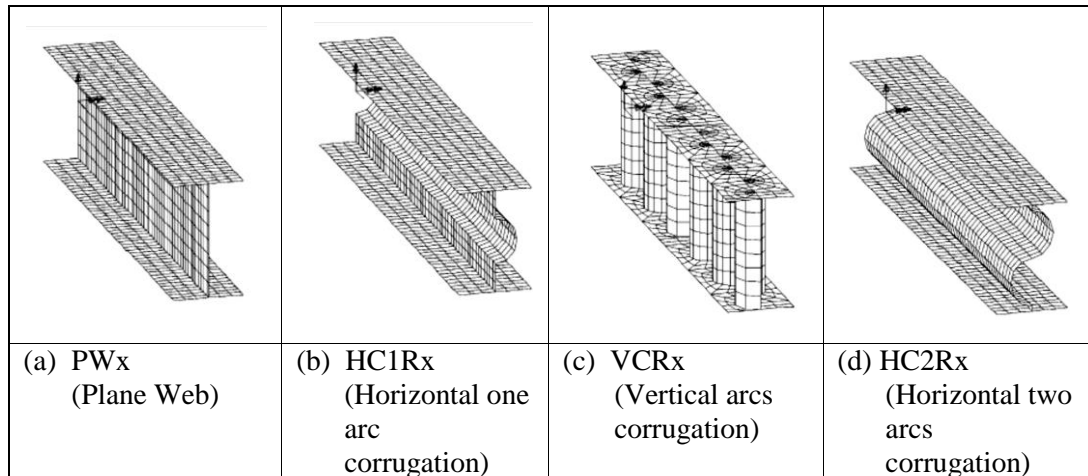


Figure 2.2 Corrugation profiles for the type of beam investigated (Chan et al., 2002)

Khalid et al. (2004) studied the bending behaviour of mild steel structural beams with corrugated web subjected to three-point bending. Semicircular web corrugation in the cross-sectional plane (horizontal) and across the span of the beam (vertical) were investigated experimentally and computationally using finite element technique. In the finite element analysis, test specimen was modelled using commercially available finite element software LUSAS and a non-linear analysis was performed. Corrugation radius of 22.5 mm thickness, with constant corrugation amplitude to cycle length ratio ( $H/\lambda$ ) and flange thickness 6 mm were selected at the base sizes. The flat web beams, welded and ordinary rolled, were also tested with both methods to develop the benchmark results. Five models of beams were selected for the experimental tests. The detail dimensions of these tests are shown in Figure 2.3. The comparisons between the experimental and the finite element analysis results were satisfactory.

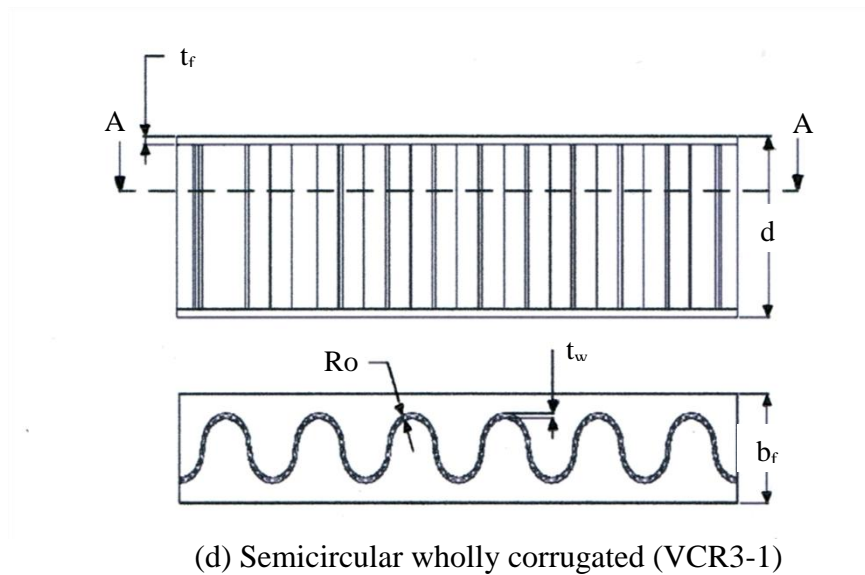
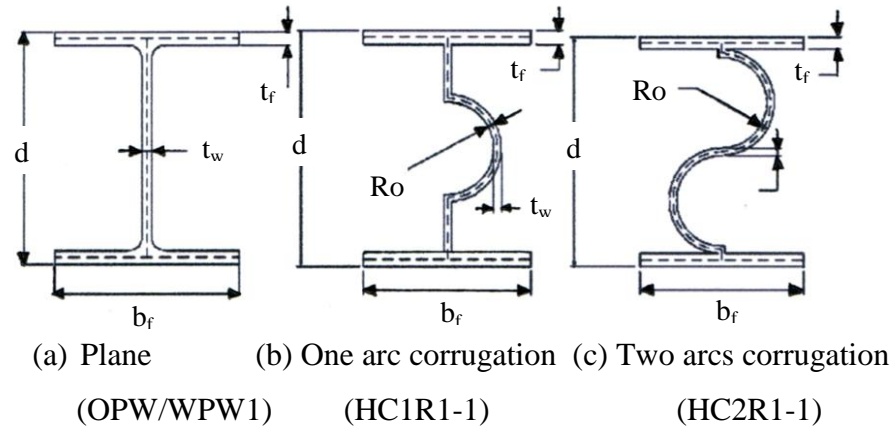


Figure 2.3 Geometry of the models tested experimentally (Khalid et al., 2004)

It was observed that the specimens gradually bend until the compression flange yielded and subsequently buckled vertically into the crippled web. The web crippling failure was not significantly seen from the HC2R1-1 and VCR3-1 specimens. It was noted that the vertical-corrugated web beam (VCR) could carry between 13.3% and 32.8% higher moment compared to the plane and horizontal-corrugated web beams. Besides that, larger corrugation radius could resist higher bending up to the yielding stage. This gives effect to the increment of the second moment of area ( $I$ ) that had

influence on the direct bending stresses ( $\sigma_{zz}$ ). In addition, reduction in weight could be achieved by using the vertical-corrugated web with the maximum size of corrugation radius. This was true for the corrugation shapes and sizes taken.

Luo and Edlund (1996a) performed nonlinear finite element analysis to study the effect of strain hardening model, corner effect, initial imperfection (local and global), loading position, load distribution length and variation of geometric parameters. Elastic-perfectly plastic model and Ramberg-Osgood's model were used to analyze the first factor. It was found that with a Ramberg-Osgood strain-hardening model for webs, the ultimate strength of the girder is about 8%-12% higher than the ultimate strength with an elastic-perfectly plastic model. A block distribution of the yield stress was used to study the corner-effects, and it was found that the yield stress and the degree of strain hardening for the material in a small region around the corner of the web profile is higher than in other regions.

For initial imperfections of the girder, it was found that small global initial imperfection does not have much effect on the behavior and load-carrying capacity of the girder, while local initial imperfection results in a notable reduction of nearly 7% in the ultimate load. As far as the load position is concerned, the influence of three loading positions as shown in the Figure 2.4 was considered. The highest value of strength is obtained when the girder is loaded at the centre of the oblique part of corrugation whereas the girder has the lowest ultimate load when the load is applied at the centre of the flat part. The load distributions also affected the failure load of the girder. Patch load apparently resulted in a much higher ultimate load than that under knife load. It was observed that the ultimate load for a girder subjected to a knife-load is about 40% and 20% lower than that when the knife-load was replaced by a uniformly distributed patch

load with length,  $c = 115.2$  mm and 50 mm respectively. Besides that, the performance of corrugated girders can be affected by the corrugation parameters. Girders with larger corrugation angle and thicker web and flange have higher ultimate strength or ultimate shear capacity. In addition, the shear capacity increases proportionally with the girder depth but an insignificant effect on the ultimate strength was observed when subjected to patch load. The panel dimension  $H$  and  $L$  as shown in Figure 2.5 do not effect on the ultimate strength for girders with  $t_f = 10$  mm, except when  $H$  is extremely small ( $\leq \approx 200$  mm) (Luo and Edlund, 1996a).

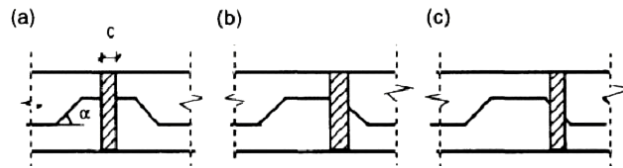
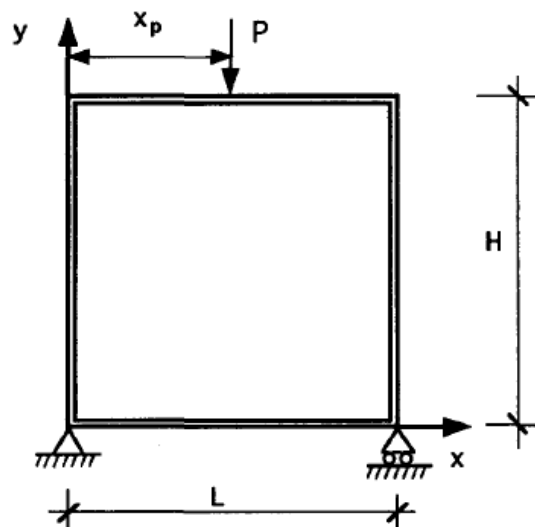
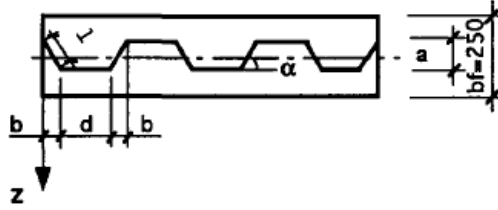


Figure 2.4 Types of loading positions (Luo and Edlund, 1996a)



(a) The girder and the load

Figure 2.5 A steel girder with trapezoidally corrugated webs under patch loading (Luo and Edlund, 1996a)

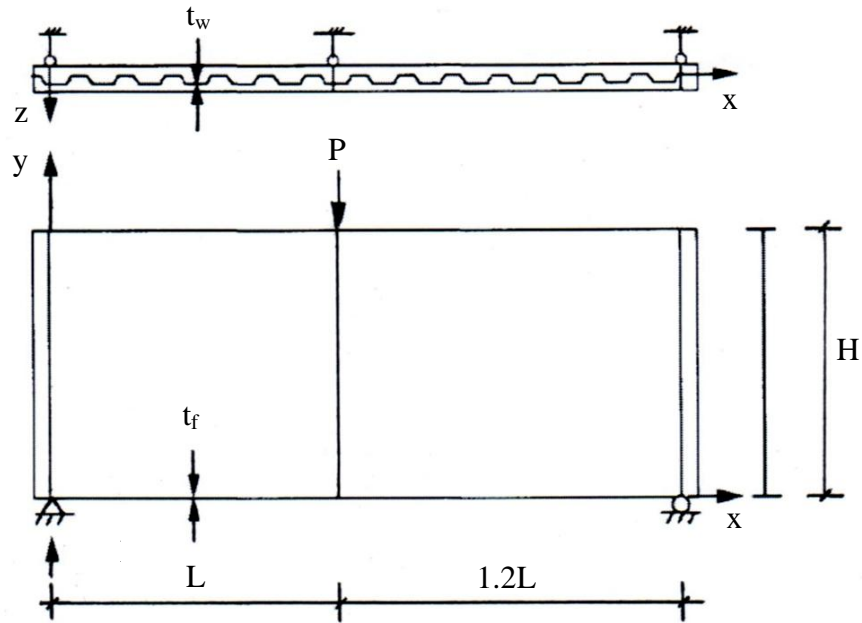


(b) The geometry of the web and the flange

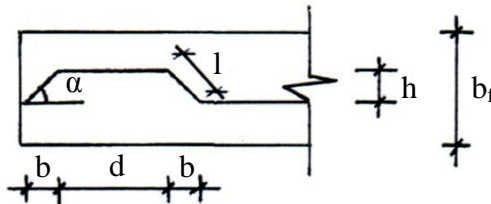
Figure 2.5 (continued)

Luo and Edlund, (1996b) used non-linear finite element analysis to perform a geometrical parametric study and compared the numerical results with existing empirical and analytical formulae. Within the parametric range studied (see Figure 2.6), the ultimate shear capacity increases proportionally with the girder depth and seems not to be dependent on the ratio of girder length over girder depth ( $L/H$ ), while the post-buckling shear capacity not only increases with the girder depth, but also dependent on the ratio of girder length over girder depth. The ultimate and the post-buckling shear capacity increase as the web thickness increases but not proportional to the cube of the web thickness. The corrugation depth did not have much effect on the ultimate shear capacity but affected the degree of the localization of the buckling mode. Besides that, shear capacity increases slightly as the corrugation angle increases from  $30^\circ$  to  $60^\circ$ . The buckling mode changes from a global buckling mode for  $\alpha = 30^\circ$ , to a zonal buckling mode for  $\alpha = 45^\circ$  and to a more localized buckling mode for  $\alpha = 60^\circ$ . Other geometric parameters that had been studied were flat sub-panel width,  $b$ , which the ultimate and the post-buckling shear capacity decrease as the flat sub-panel width  $b$  increases. It can be concluded the reduction of the shear capacity and the post-buckling shear capacity is in the average of about 20%-30% of the ultimate shear capacity.





(a) The geometry and loading



(b) Notation of corrugation and flange geometry

Figure 2.6 A plate girder with trapezoidally corrugated webs in shear (Luo and Edlund, 1996b)

Sayed-Ahmed (2005a) investigated the behavior of corrugated steel webs, the different buckling modes, the interaction between the yield failure criterion and buckling modes and proposed an interaction equation considering the different failure criteria including steel yielding. It was found that the panel width had the most significant effect on the mode of buckling. An ideal ratio between the inclined panel width and the horizontal panel width for a trapezoidal corrugation profile is proposed to be 1.0.

Besides that, global buckling mode governs the instability behavior for significantly small corrugation width  $b$  (dense corrugation) and the local buckling mode governs the behavior for significantly large values of  $b$ . The corrugation angle also affects the interactive critical stress for small panel widths,  $b$  where the behavior of the corrugated web is governed by either pure global buckling or interaction between global buckling and steel yielding. Then, the nonlinear finite element model was extended to investigate the post-buckling strength of corrugated web girders. The numerical analysis reveals that girders with corrugated steel webs continue to carry loads after web buckling is encountered. The post-buckling strength of corrugated web girders was highly dependent on the panel width. For corrugated webs with larger panel widths, the post buckling strength may reach 53% for a 400 mm panel width. It was concluded from the numerical analysis that resistance to lateral torsion-flexure buckling of such girders is 12% to 37% higher than the resistance of plate girders with traditional plane webs to lateral buckling (Sayed-Ahmed, 2005b).

In steel design, the second moment of area about y-y axis,  $I_y$  is important as it has an effect on the lateral torsional buckling resistance of a TWP steel section. An experimental study was carried out to determine the elastic load-deflection behaviour of steel sections containing flat web and TWP of the same dimensions (Denan, 2008). The dimensions of the sections are 170×100×9×4 mm and 200×80×5×2 mm. The objective of the tests was to obtain the flexural stiffness ( $P/\delta$ ) of TWP and FW steel sections. These were then used to obtain the  $I_x$  and  $I_y$  values of the TWP sections. The vertical deflection readings were recorded in all tests. A total of 24 elastic bending tests were carried out. The results of the study indicate that the  $I_y$  of TWP is in the range of 1.28% to 6.57% more than the  $I_y$  of FW. However, the value of  $I_x$  for the TWP section is in the

range of 11.51% to 16.54% lower than the  $I_x$  of the FW. In summary, the TWP steel section has a higher stiffness in minor axis compared to the FW but has lower stiffness in major axis. Denan et al. (2009) studied the second moment of area in major ( $I_x$ ) and minor ( $I_y$ ) axes of TWP steel sections and present the results of an experimental investigation.

The ability of a wholly corrugated web (WCW) H-beam to resist buckling have been studied quantitatively by Zhang et al. (2000) and Li et al. (2000) which involves the influence of the corrugation parameters. A set of optimized parameters were developed for the WCW based on basic optimization of the plane web beams. It was found that the corrugated web beam had 1.5-2 times higher buckling resistance than the plane web beam. The WCW can enhance greatly the stability of the web to resist pressure and the ability to resist buckling better than plane web beam. The structure feature of the WCW H-beam is shown in Figure 2.7, with periodic corrugations along the direction of the web length.

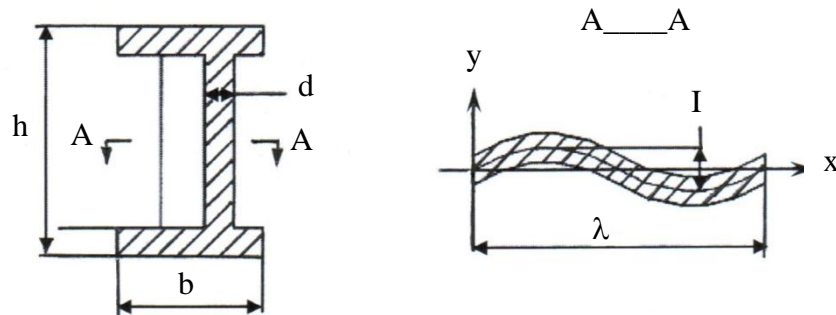


Figure 2.7 Structural character of the WCW H-beam (Zhang et al., 2000; Li et al., 2000)

Osman et al. (2007) carried out an experimental work on a composite beam with trapezoidally corrugated web steel section to study its structural performance in elastic

and plastic stage in comparison with the composite beam with FW. For comparison, a full scale composite beam test specimen with trapezoidal steel section and with FW section was tested under bending. Two specimens of 5 m in length with steel section of 300×120 mm and concrete section of 110×1000 mm were tested. Sufficient stud connectors were provided to give full interaction between the steel and concrete. Deflections behavior under loading, position of neutral axis, distribution of strain across the depth of the composite section were measured and analysed. It was found that, in elastic state, the contribution of trapezoidal web in TWP-composite beam in resisting tension is too small and can be neglected. This is because the tension force resistance is only concentrated at the flanges of TWP steel section, causing the bottom flange to yield earlier than the normal FW beam. This was based on the analysis of strain distribution and the position of the neutral axis in both beam specimens. In the elastic-plastic region, especially after the bottom flange reached its yield strength, TWP section shows a better performance with less deflection and the web is stiffer at buckling. The results show that the composite beam with trapezoidal web has no significant difference in its structural performance at elastic stage compared to the composite beam with normal FW.

Recently, Yi et al. (2008) studied the nature of the interactive shear buckling of corrugated webs (Figure 2.8), and concluded that the first order interactive shear buckling equation that does not consider material inelasticity and material yielding provides a good estimation of the shear strength of corrugated steel webs. The geometric parameters affecting the interactive shear buckling was determined as  $a/h$  and  $d/t$ . As conclusion,  $a/h < 0.2$  and  $d/t > 10.0$  were proposed as the limit conditions for the corrugated webs. Later, shear strength and design criteria of trapezoidally corrugated webs, based on the first order interactive equation proposed by Yi et al. (2008) were then